Shapes Recognition Using the Straight Line Hough Transform: Theory and Generalization

Derek C. W. Pao, Hon F. Li, *Member, IEEE*, and R. Jayakumar

A shape matching technique based on the straight line Hough transform (SLHT) is presented. In the θ-ρ space, the transform can be expressed as the sum of two terms, namely, the *translation term* and the *intrinsic term*. This formulation allows the translation, rotation, and intrinsic parameters of the curve be easily decoupled. A shape signature, called the *scalable translation invariant rotation-to-shifting* (STIRS) signature, is obtained from the θ-ρ space by computing the distances between pairs of points having the same θ value. This is equivalent to computing the perpendicular distances between pairs of parallel tangents to the curves. This signature has the following properties: 1) It is invariant to translation; 2) rotation in the image space corresponds to circular shifting of the signature; 3) the signature can be easily normalized. Matching two signatures only amounts to computing a 1-D correlation. The height and location of a peak (if it exists) indicates the similarity and orientation of the test object with respect to the reference object. Knowing the orientation, the location of the test object is obtained by an inverse transform (voting) from the θ-ρ space to the x-y plane. Examples demonstrating the feasibility of these techniques are presented.

The shape matching technique assumes that the shape is characterized by its set of tangent lines. It is proved, based on curve reconstruction, that a continuous closed smooth curve is indeed uniquely characterized by its complete set of tangents. This result serves as the theoretical foundation of the shape recognition methodology based on SLHT.

Index Terms— **Parameter space decomposition, shape matching, STIRS signature, straight line Hough transform, tangent set representation.**

I. Introduction

THE HOUGH transform (HT) is a well-known method for the detection of parametric curves in binary images [1], [7], [9]. However, high computational cost poses severe restrictions on its applicability to large images. One effective approach to overcome this drawback is the parameter space decomposition [19]. In this approach, the high dimensional parameter space is decomposed into several lower dimensional subspaces such that parameters of individual subspaces can be determined sequentially. In order to decompose the parameter space, we have to formulate the transform in such a way that parameters can be easily decoupled. One technique to achieve this is by first computing the straight line Hough transform (SLHT) in the θ-ρ space and then computing transforms from the θ-ρ space to the decomposed parameter subspaces [5], [14].

Manuscript received June 13, 1990; revised January 21, 1992. This work was supported by the NSERC and FCAR. Recommended for acceptance by Associate Editor S. Tanimoto.

The authors are with the Department of Computer Science, Concordia University, Montreal, Quebec, Canada H3G 1M8.

IEEE Log Number 9202382.

In the θ-ρ space, the transform can be expressed as the sum of two terms, namely, the *translation term* and the *intrinsic term*. One major advantage of formulating the transform in the θ-ρ space is that the translational parameters can be easily separated, and rotation in the image space only corresponds to circular shifting in the θ-ρ space. The techniques presented in [15] for the detection of ellipses achieve better asymptotic complexity compared with other Hough-based techniques.

In this paper, we address two fundamental issues of the SLHT. First, we generalize and extend the method to recognize arbitrary shapes. Conceptually, each point in the θ-ρ space corresponds to a line that is tangent to the curve. A second transform is computed by measuring the perpendicular distances between pairs of parallel tangent lines. This can be done simply by computing the distances between pairs of points in the θ-ρ space that have the same θ value. The second transform, which is a signature of the shape, possesses the following three properties: 1) invariant to translation, 2) rotation in image space corresponds to circular shifting of the transform, and 3) the scaling factor of the shape can be easily normalized. To recognize the test object, we need only to compute a 1-D correlation of the signature with the normalized reference signature. The location of a peak also indicates the orientation of the object. Based on the estimated orientation, we determine the translation term of the test object in the θ-ρ space by performing another column by column 1-D correlation of the SLHT transform of the reference object with the transform of the test image. The coordinates of the location of the test object is then obtained by an inverse transform of the translation term. The computational complexity of this method is very attractive.

The second issue is the uniqueness of the SLHT. In this paper, we prove that the SLHT transform of a continuous closed smooth curve is unique. In the continuous domain, this problem is equivalent to proving the uniqueness of the complete set of tangents of a continuous closed smooth curve. Let C_1 and C_2 be two continuous closed smooth curves in the x-y plane, and let $H(C_1)$ and $H(C_2)$ be the complete set of tangents of C_1 and C_2, respectively. We will prove that $H(C_1) = H(C_2)$ if and only if $C_1 = C_2$. This uniqueness problem is also of interest in geometry [8]. In this paper, we will present a proof that relaxes the assumption on the existence of the second derivative of the curve that was made in the proof of [8]. This result serves as the theoretical foundation of the pattern recognition methodology based on SLHT.

In the next section, we will first introduce the SLHT transform and the shape signature. Detailed matching algorithms

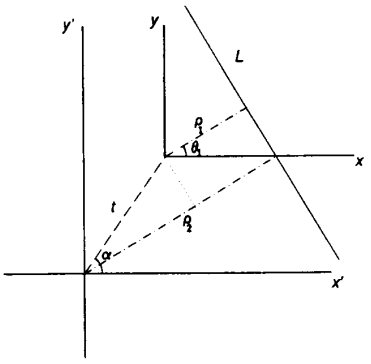

Fig. 1. Effect of translation on the normal parameters of a straight line.

and examples will be presented. Some performance aspects, for example, the time complexity, noise and quantization errors, multiple objects, and occlusion will be discussed. In Section III, we will present a detailed proof of uniqueness of the SLHT transform of closed smooth curves. Concluding remarks and future research issues are discussed in Section IV.

II. Recognition of Arbitrary Shapes

A. SLHT Transform of a Curve

In the recognition of arbitrary shapes, we are concerned with the detection of the object as well as the estimation of the amount of translation, rotation, and scaling of the object in the image. The SLHT transform of a shape, say C, is the set of lines that are tangent to it. The transform can be regarded as a multiple-valued function $\rho(\theta)$, which is a mapping $\theta \rightarrow \rho$, such that for a given θ, say θ_i, $\rho(\theta_i) = \{\rho_k |$ the line $l : \rho_k = x\cos\theta_i + y\sin\theta_i$ is tangent to $C\}$.

First, we consider the effects of translation and rotation on the transform of a single straight line $l = (\theta_1, \rho_1)$. If the image plane is rotated by an angle $\phi < 180°$ in the counterclockwise direction,[1] then the point (θ_1, ρ_1) will be mapped to (θ_2, ρ_2) such that

$$\theta_2 = (\theta_1 + \phi) \bmod 180° \text{ and } \rho_2 = \begin{cases} \rho_1 & \text{if } \theta_1 + \phi < 180° \\ -\rho_1 & \text{if } \theta_1 + \phi \geq 180°. \end{cases}$$

If the image plane is being translated by (x_0, y_0) (refer to Fig. 1), then

$$\theta_2 = \theta_1 \text{ and } \rho_2 = t\cos(\theta_1 - \alpha) + \rho_1$$

where $t = \sqrt{x_0^2 + y_0^2}$, and $\alpha = \tan^{-1}(y_0/x_0)$.

Let $\rho_0(\theta)$ denote the SLHT transform of a curve C located at the origin. If C' is a scaled, rotated, and translated instance of C, the SLHT transform of C' is given by

$$\rho(\theta) = t\cos(\theta - \alpha) + S * sign * \rho_0(\theta - \phi)$$

where S is the scaling factor; $sign = 1$ if $\theta \geq \phi$; otherwise, $sign = -1$. The "+" operator means adding the value of $t\cos(\theta - \alpha)$ to every element in $\rho_0(\theta - \phi)$. The $t\cos(\theta - \alpha)$ term is called the *translation term*, and the $\rho_0(\theta - \phi)$ term is called the *intrinsic term*. We can see that this representation provides a natural decomposition of the parameter space. If we can eliminate either one of the two terms in the transform, determining the parameters of the term left behind is relatively easy. In [14] and [15], novel techniques had been developed to detect parametric curves, such as circles and ellipses. The parameter space is decomposed into three subspaces, namely, the translational space, rotational space, and the intrinsic space (which consists of parameters other than the translation and rotation parameters). In our approach, we first eliminate the intrinsic term of the transform function by selecting multiple number of points in θ-ρ and then compute a voting in the t-α space to determine the location of the curves. This approach only requires searching a 1-D space of the orientation, and its computational complexity is better than other Hough-based methods. In this paper, we further generalize the approach to detect arbitrary shapes.

B. Shapes Matching Using the STIRS Signature

In the discrete domain, we compute the SLHT transform for a finite number of values of θ. If the θ and ρ axes are quantized into m_θ and m_ρ levels, respectively, the transform can be represented simply by a 2-D (boolean) array of size $m_\theta \times m_\rho$. One important observation of the transform is that the same offset value, namely, $t\cos(\theta_i - \alpha)$, is added to all points in the θ_ith column of the array. One simple way to eliminate the translation term is by measuring the distances between pairs of points of the array that are in the same column. Conceptually, this is equivalent to computing the perpendicular distances between pairs of parallel tangent lines of the curve. The resultant transform is then a *signature* of the shape. This signature possesses the following three properties:

1. It is invariant to translation of the shape in the image plane.
2. Rotation of the shape in the image plane corresponds to circular shifting of the signature.
3. If the shape is scaled by a factor S in the image plane, then the signature will also be scaled by the same factor.

We call this the *scalable translation invariant rotation-to-shifting* (STIRS) signature.[2] Matching a test signature with a reference signature only involves computing a 1-D correlation of the two templates. The location of the peak will also indicate the orientation of the shape with respect to the reference shape.

There are several possible ways to define the STIRS signature depending on how the pairs of points are selected. Three choices are as follows:

- C1: Select all possible combinations of pairs of points that belong to the same column.
- C2: Select pairs of points such that one of the points has the maximum or minimum ρ value (index) in the column.
- C3: For each point, say p_i in the θ_jth column, select at random at most c (a small constant) distinct points in the same column, say p_j for $j = 1$ to c, and compute

[1] If $\phi \geq 180°$, then we can perform the rotation in two steps $\phi_1, \phi_2 < 180°$ and $\phi = \phi_1 + \phi_2$.

[2] In general, the STIRS signature is not unique. For example, the STIRS signatures of all convex objects of constant width [6] are equal to a horizontal line in θ-ρ.

the distances between the pairs of points p_i and p_j. If the scaling factor is known, then we can add one more constraint in selecting the points such that the distances between any selected pair of points should be less than or equal to the diameter of the reference pattern.

Intitutively, C1 is most attractive because it captures maximum information. However, for complex shapes and composite shapes, the signature may allow too many less prominent features to appear and create confusion among shapes. In C3, random pairs of points are selected. Hence, the signature may not contain all the features of the shapes in the test image. Thus, C2 is a good compromise between C1 and C3. However, the signature will then become more sensitive to distortions or occlusions that affect the convex hull of the shape (this is because the tangents with minimum or maximum value of ρ correspond to the supporting half plane of the convex hull of the composite shape). For complex images that contain multiple objects, computing the signature using the second definition may result in a signature that is totally different from the signature of any of its composite shapes. It is because the convex hull of the composite shape will be very different. Hence, the following strategy is adopted: signatures of the reference shapes (known shapes) are computed using C2, and signatures of complex test images are computed using C3. When multiple shapes are present in the test image, the test signature computed using C3 will contain some features of each of its constituent components.

1) Matching Algorithms: The procedure to recognize an object is as follows:

Step 1: Compute the $\rho(\theta)$ transform and the signature of the test pattern.

Step 2: Normalize the reference signature with respect to the test signature. If the image contains multiple objects, and the scaling factor is not known, then a coarse-to-fine search is performed.

Step 3: Determine the orientation of the object by computing a 1-D correlation of the reference signature with the test signature. If no significant peak is detected, then we can conclude that the test pattern is not an instance of the reference object. The position of the peak indicates the amount of rotation ϕ (or $\phi + 180°$ since the signature is periodic in 180°) of the test pattern.

Step 4: Eliminate the intrinsic term in $\rho(\theta)$ by "subtracting" the scaled and shifted reference transform $S * sign * \rho_0(\theta - \phi)$. Since $\rho(\theta)$ is a multiple-valued function, the subtraction is basically a correlation between the two "vectors" $\rho_0(\theta_i - \phi)$ and $\rho(\theta_i)$ for each θ_i. We will elaborate on this later. The translation parameters can then be determined by an inverse transform to the x-y plane [5] or by performing a voting in the x-y plane. The peak corresponds to the location of the test pattern in the image plane. If no peak is found, then the test pattern is not an instance of the reference object.

The SLHT transform of the test image is computed using the modified Hough transform algorithm developed in [11]. The modified algorithm checks for pixel connectivity, and each detected segment is a continuous string of pixels. In this paper, we regard the θ-ρ space as a boolean array $A[0 \ldots m_\theta][0 \ldots m_\rho]$, such that $A[\theta_j][\rho_i]$ will have a value of 1 if the corresponding accumulator cell contains one or more detected line segments; otherwise, the entry will have a value 0. The signature is also represented by a 2-D array $D[0 \ldots m_\theta][0 \ldots m_\rho]$ such that $D[\theta_j][\rho_i] = 1$ if the distance between a selected pair of points in the θ_jth column is equal to ρ_i; otherwise, $D[\theta_j][\rho_i] = 0$. To find out the rotation of the test pattern, we simply slide the reference signature (with wraparound) over the test template. The position at which maximum correlation occurs corresponds to the amount of rotation ϕ (or ϕ+180°). The detailed algorithm is listed below, where D_0 and D_t are the signatures of the reference object and the test image, respectively. In the matching algorithm, a higher weighting is given to the case when more than one pixel in the same column of the reference template match the pixels in the test template.

Matching Algorithm

```
/* h2[] = accumulated scores due to exact matches
 h1[] = accumulated scores due to approximate matches
 miss[] = accumulated penalty due to misses
 */

FOR θ1 := 0 to mθ −1
begin
 FOR θ2 := 0 to mθ −1
 begin
  t := (θ2 − θ1) modmθ;
  c1 := c2 := m := 0;
  FOR ρ1 := 2 to mρ/2
  begin
   IF (Dt[θ1][ρ1] = 1)
   begin
    IF (D0[θ2][ρ1]) = 1)
     c2 := c2 + 1;
    ELSE IF (D0[θ2][ρ1 ± 1] = 1)
       c1 := c1 + 1
     ELSE
       m := m + 1;
   end
  end;
  /* more weight is given to the case when multiple number
of points match */
   h2[t] := h2[t] + c2 * c2;
   h1[t] := h1[t] + (c1 * c1)/2;
   miss[t] := 2 * m;
 end
end;
/* normalize the score; count = number of points in D0 */
FOR t := 0 to mθ − 1
 score[t] := (h2[t] + h1[t] − miss[t]) * 100 /count;
detect peak in score[t];
```

The time complexity of this process is $O(m_\theta{}^2 m_\rho)$. However, we can easily improve the efficiency by adopting compact storage for D_0 and D_t. The time complexity may then become $O(m_\theta{}^2 K_D)$, where K_D is the average number of

points in each column vector of D_0 and D_t. Once we know S and ϕ, we can determine the translation parameters by "subtracting" $S * sign * \rho_0(\theta)$ from $\rho(\theta)$. Recall that the effect of translation is the same as adding the offset $t\cos(\theta_i - \alpha)$ to each element of $\rho_0(\theta_i)$. Determining the value of the offset is equivalent to finding the position at which maximum correlation of the two vectors $A_0[\theta_i]$ and $A_t[\theta_i]$ occurs, where A_0 is the *intrinsic* transform of the reference shape, and A_t is the transform of the test image. The correlation is similar to that described in the matching algorithm. The only difference is that we now have 1-D vectors instead of 2-D templates. Let $T[m_\theta]$ denote the resultant translation term obtained for each θ_i. In case there is no significant correlation between the two vectors, the corresponding entry in $T[m_\theta]$ will be set to *nil*. The translation term, which is a sinusoidal curve, is equivalent to the SLHT transform of a single point in the image plane. To determine the amount of translation (i.e., the coordinates of the reference point), we can perform an inverse transform to the x-y plane [5]. Each point in θ-ρ is mapped into a straight line in x-y, and the point in x-y having the highest vote count is the inverse transform of the sinusoidal curve in θ-ρ. A more efficient approach is to perform a voting in the x-y space by selecting pairs of lines (points in θ-ρ) and vote only for the intersecting point of the two lines. The latter approach is used in the examples presented in Section II-C.

2) Computational Complexity: In this section, we analyze the overall complexity of the matching process. Assuming that the input image is of size $N \times N$ and the number of black pixels is P (the length of the object contour), the computational complexity of our method can be divided into two parts, namely, the overhead and the matching cost. The overhead includes computing the transforms and filtering the θ-ρ space. To simplify the comparison, we assume that the algorithms are implemented in a sequential machine. To implement the SLHT transform described in Section II-A, we need to sort the pixels. This can be done by simply reading out the pixels in row major or column major order. Hence, the complexity to compute the SLHT is $O(N^2 + Pm_\theta)$. The time to compute the STIRS signature is $O(m_\theta k)$, where k is the average number of points in each column of $\rho(\theta)$. Hence, the total overhead is $O(N^2 + Pm_\theta + m_\theta k)$, which is approximately equal to $O(N^2 + Pm_\theta)$.

The algorithm to match STIRS signatures takes $O({m_\theta}^2 K_D)$ time, where K_D is the average number of points in each column of the reference signature, and the time required to compute the translation term is $O(m_\theta k)$. Finally, the voting algorithm to determine the translational parameters has a complexity of $O(m_\theta K_D + N^2)$, where N^2 is the time to locate the peak in the x-y plane. Suppose there are η different object classes. To determine the class of a test pattern, we only need to match the signature of the test pattern with the η reference signatures. Assume that only one reference template matches with the test pattern; then, the total matching cost is $O(\eta m_\theta^2 K_D + m_\theta K_D + m_\theta K_D + N^2)$ which is approximately equal to $O(\eta {m_\theta}^2 K_D)$.

For comparison purposes, we now consider the standard template matching and the GHT [1]. In the standard template matching, there is no overhead involved. Let the template size be $T \times T$, and let the search range of the allowable translation be R. Then, the matching cost of this method is $O(\eta m_\theta R^2 T^2)$, where R^2T^2 is at least $O(N^2)$.

In the GHT, the gradients of each contour pixels are first computed. Let κ be the average number of pixels having the same gradient, i.e., $\kappa = P/m_\theta$. Then, the matching cost of GHT is $O(\eta(m_\theta P\kappa + \text{cost of peak detection in image plan}))$. Assume that the votes are mapped to a region in the image plane of size $n \times n$. Then, the complexity is equal to $O(\eta(P^2 + n^2))$.

Comparing the above three methods, our method involves an additional feature extraction phase (computing the signature). Because of the invariant properties of the signature, the matching cost of our method is much lower than the other two methods. The advantage of our method is even more prominent when the number of object classes η is large.

3) Noise and Quantization Errors: There are two sources of quantization errors: the digitization of the image plane and the quantization of the θ-ρ space. In digital images, the notion of "smoothness" is not well defined. The resolution of the digitization will determine how well we can estimate the gradient of the curve. This problem is further complicated by the quantization of the θ-ρ space. Because of discretization, spreading of long straight line segments across adjacent accumulator cells is very common [17]. In order to capture the tangents at places with small radius of curvature, a lower threshold should be used. However, lowering the threshold will certainly increase the noise (spurious tangents) in the transform space due to spreading of straight line segments. Two suggestions for overcoming this problem are proposed:

1. To reduce the noise in the θ-ρ space due to spreading of straight line segments across two or three adjacent accumulator cells, we can lump connected line segments in adjacent buckets of the same column (same θ) into one. This can be done since the information about the end points of the line segments are available. The effective value of ρ is taken as the weighted average, where the length of the line segment is used as the weight.
2. To remove spurious tangents, we can first extract long straight lines from the θ-ρ space. The selected straight lines are then reconstructed. Any line segment in θ-ρ whose length is less than some threshold L_t will be removed if its constituent pixels are included in the reconstructed image.

The first filtering technique was incorporated in the example shown in Section II-C.

Although the SLHT may suffer from quantization errors, the technique is very robust against random noise in the image. This is because when we compute the SLHT transform, pixel connectivity is checked, and single pixels (random noise) will be discarded.

C. Examples

The examples presented are only aimed at illustrating the basic idea of the approach. Figs. 2(a) and 3(a) show two reference shapes S1 and S2, respectively. The size of the

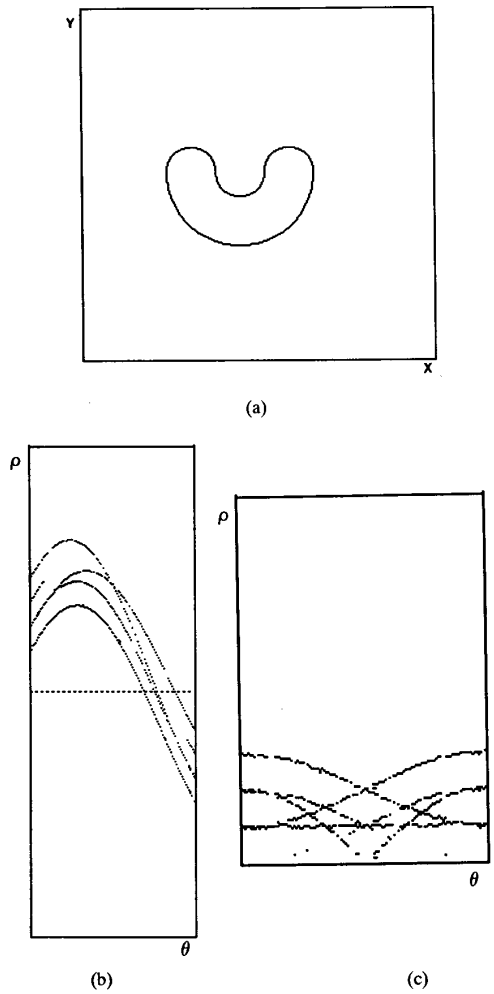

Fig. 2. (a) Reference shape S1; (b) SLHT transform of S1; (c) STIRS signature of S1.

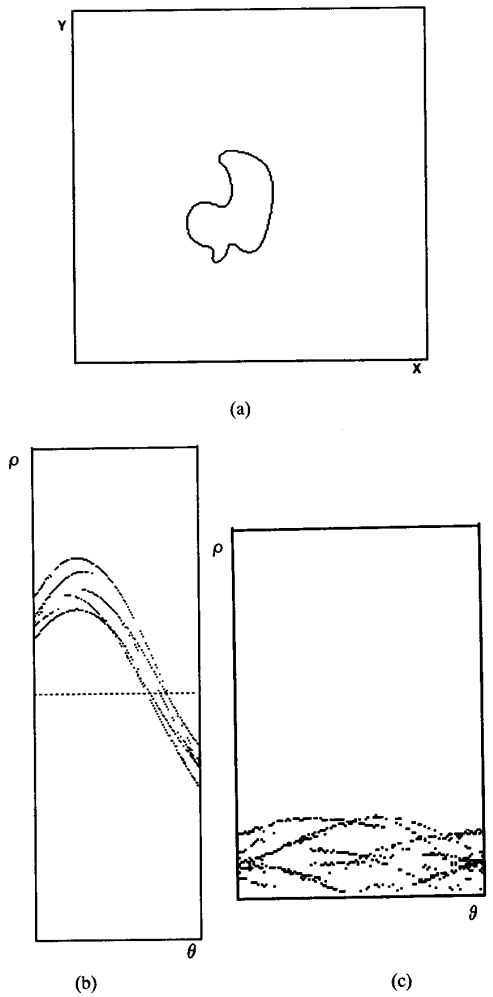

Fig. 3. (a) Reference shape S2; (b) SLHT transform of S2; (c) STIRS signature of S2.

images are 256×256. The center of mass of the reference shapes are used as the reference point of the shape; hence, the locations of S1 and S2 in the reference images are at (114,119), and (115,110), respectively. We compute the SLHT transform of the images with the following parameters: $\Delta\rho = 2.0$, $\Delta\theta = 1.5°$, and line segments with length less than five units are discarded. The SLHT transform and the STIRS signature of S1 and S2 are also shown in the figures. The θ-ρ plane is divided into two halves by the dotted line in the plot, the upper half corresponds to positive ρ's, and the lower half corresponds to negative ρ's. The signatures of the reference shapes are computed using C2. Fig. 4(a) shows a test image consisting of rotated (transposed) and translated instances of S1 and S2. The STIRS signature of the test image is computed using C3, and each point is paired with two to three other points in the same column. The result of matching the reference signatures against the test signature is shown in Fig. 5. The orientations of the patterns in the test image are correctly determined. Based on the estimated orientation, the translation term of the two test patterns are obtained by performing a column-wise correlation between the intrinsic transform of the reference shapes and the SLHT transform of the test image. The intrinsic transform of the reference shapes are obtained by subtracting the corresponding translation terms $164.8\cos(\theta - 46.23°)$ and $159.1\cos(\theta - 43.73°)$ from the SLHT transforms of Figs. 2(b) and 3(b), respectively. The correlation results are shown in Fig. 6. The location of the test pattern is then determined by a voting in the x-y plane. The estimated location of the test patterns are at (87,93), and (134,117), whereas the expected values are (88,94), and (134,115), respectively. The errors in the estimated locations are acceptable since we have $\Delta\rho = 2$.

Fig. 7(a) shows a second test image that consists of shapes S1 and S2, but this time, S2 is occluded by S1. Note that a significant amount of features of S2 (angular spans along the contour) are occluded. The results of matching the reference signatures of Figs. 2(c) and 3(c) against the signature of the second test image are shown in Fig. 8. Although a

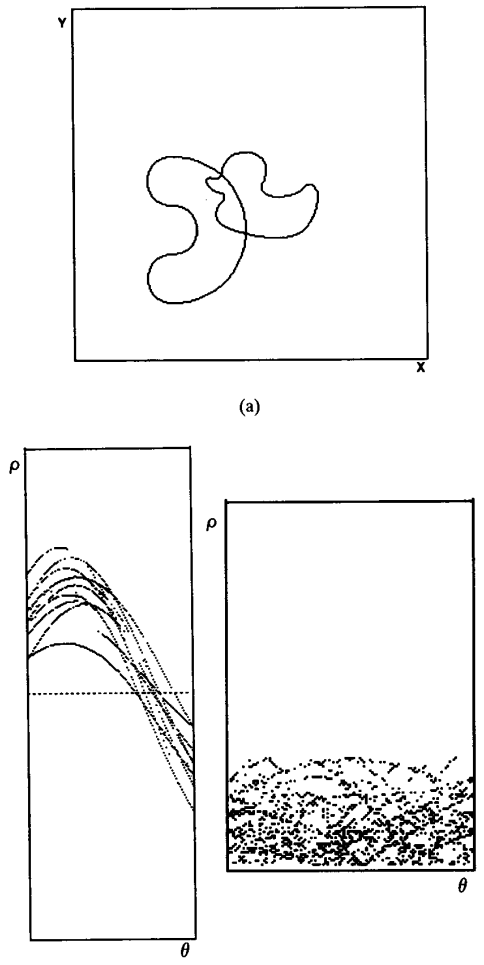

Fig. 4. (a) Test image T1; (b) SLHT transform of T1; (c) STIRS signature of T1.

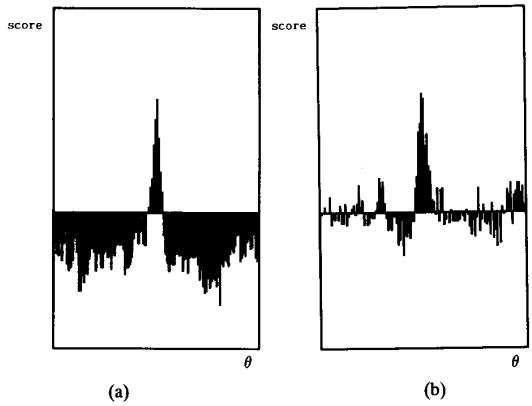

Fig. 5. (a) Result of matching the STIRS signature of S1 against that of T1; peak found at (score, θ) = (67, 90°); (b) result of matching the STIRS signature of S2 against that of T1; peak found at (score, θ) = (68.5, 89.25°).

significant part of S2 is occluded, the correlation still gives a good estimate of the orientation of S2 (offset by $\Delta\theta$). The

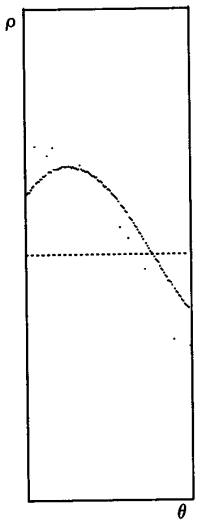

(y) \ (x)	76	78	80	82	84	86	88	90	92	94	96	98	100
80	0	0	0	0	0	0	0	0	0	0	0	0	0
82	0	0	0	0	0	0	0	0	0	0	0	0	0
84	0	0	0	0	0	0	0	0	0	0	0	0	0
86	0	0	0	0	0	0	0	0	0	0	0	0	0
88	0	0	0	0	0	2	0	3	3	0	0	0	0
90	0	0	0	1	5	18	28	29	0	0	0	0	0
92	0	0	2	4	20	98	143	15	0	0	0	0	0
94	0	0	0	6	12	47	134	12	1	1	1	0	0
96	0	0	0	0	1	3	12	4	5	0	0	0	0
98	0	0	0	0	1	2	2	0	1	0	0	0	0
100	0	0	0	0	1	0	0	2	0	0	0	0	0
102	0	0	0	0	0	0	0	0	0	0	0	0	0
104	0	0	0	0	0	0	0	0	0	0	0	0	0

(b)

Fig. 6. (a) Translation term obtained by eliminating the intrinsic transform of S1; (b) translation term obtained by eliminating the intrinsic transform of S2.

correlation result of S1 shows some improvement (a sharper peak is obtained), which is because the proportion of the points in the test signature belonging to S1 is larger than that in the first example. Based on the estimated orientations, the translation term of the two shapes are obtained as before. More noise is found in the translation term of S2, which is obtained by the column-wise correlation of the intrinsic transform of S2 with the SLHT transform of the test image. Since part of the contour of S2 is missing in the test image, the tangents corresponding to those missing points will not be present in the SLHT transform of the test image. Hence, the column-wise correlator may fail to find a good correlation between the reference vector and the test vector or may find a spurious offset at some columns. However, the location of S2 can still be correctly determined (refer to Fig. 9(d)). The accuracy of the estimated location of S2 is essentially the same as in the first example.

The correlation result of the occluded signature can be improved by the following strategy. In an image, if there is any occlusion, one of the objects will stand out completely. The signature of this object will have the best correlation with the test signature. We can then extract the points in θ-ρ that belong to that object. Then, we recompute the signature from the

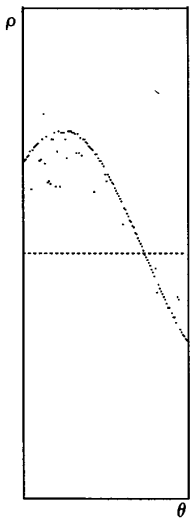

(c)

	122	124	126	128	130	132	134	136	138	140	142	144	146	(x)
106	0	0	0	1	0	0	0	0	0	0	0	0	0	
108	0	0	0	0	0	0	1	0	0	0	0	0	0	
110	0	2	4	3	2	2	3	2	0	1	0	0	0	
112	3	0	2	3	1	1	2	1	0	0	0	0	0	
114	0	1	1	0	3	9	7	0	0	0	0	0	0	
116	0	3	0	0	3	39	61	18	7	1	0	0	0	
118	0	0	0	0	3	14	80	18	5	4	1	1	0	
120	0	0	1	2	2	8	17	16	4	2	1	0	0	
122	0	0	3	0	1	4	3	0	0	1	0	0	0	
124	0	0	0	0	0	0	0	0	0	0	0	0	0	
126	1	0	0	0	0	1	0	0	0	0	0	0	0	
128	1	0	0	0	0	0	0	0	0	0	0	0	0	
130	0	0	0	0	0	0	0	0	0	0	0	0	0	

(y)

(d)

Fig. 6. (c) Results of voting on the x-y plane using the translation term in (a); (d) results of voting on the x-y plane using the translation term in (b).

segmented θ-ρ space. By successive peeling of the occluding (but not occluded) object, we can improve the correlation result of the remaining occluded objects. This is because the proportion of the points in the revised test signature that belong to the occluded objects will become larger.

D. Remarks

There are other boundary descriptors that are also translation invariant, for example, the ψ-S curve (see ch. 8 of [2]). Rotation in the image plane corresponds to circular shifting in the ψ axis. However, in performing a matching in the ψ-S space, the S axis of the test pattern and the reference pattern must also be properly aligned. Therefore, the matching process essentially involves computing a 2-D correlation.

The discrete version of the ψ-S representation is the shape number [4], which is obtained from the differential chain code of the curve boundary. In the discrete domain, the alignment of the test pattern and the reference pattern can be achieved by normalizing the number by rotating the digits until the number is minimum (or maximum). To perform matching, the shape numbers of the test and reference pattern have to be of the same order (length). The degree of similarity for two shapes is the largest order for which their shape numbers are equal.

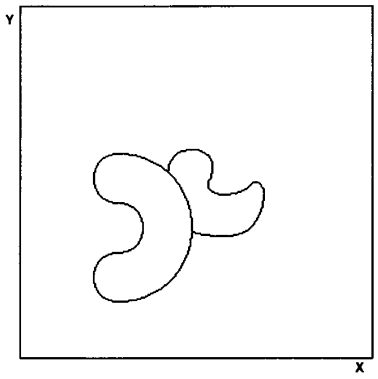

(a)

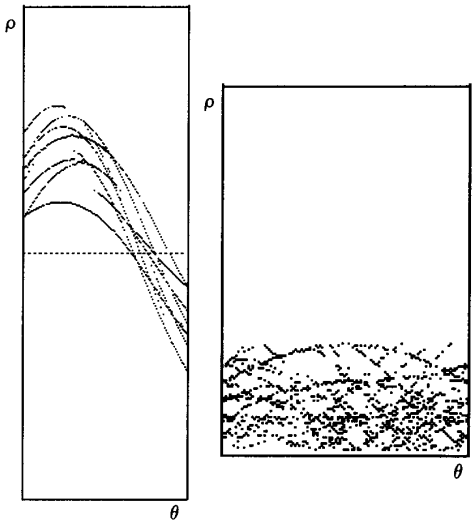

(b) (c)

Fig. 7. (a) Test image T2; (b) SLHT transform of T2; (c) STIRS signature of T2.

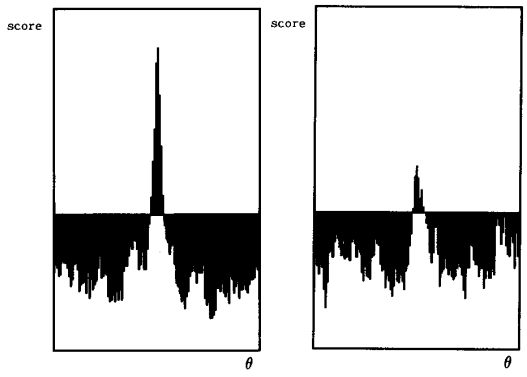

(a) (b)

Fig. 8. (a) Result of matching the STIRS signature of S1 against that of T2; peak found at (score, θ) = (98, 90°); (b) result of matching the STIRS signature of S2 against that of T2; peak found at (score, θ) = (27, 88.5°).

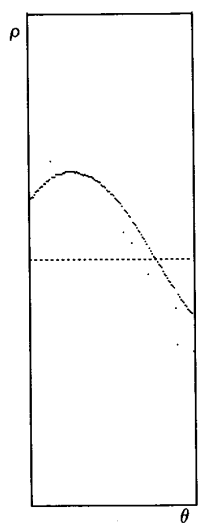

(a)

	76	78	80	82	84	86	88	90	92	94	96	98	100	(x)
80	0	0	0	0	0	0	0	0	0	0	0	0	0	
82	0	0	0	0	0	0	0	0	0	0	0	0	0	
84	0	0	0	0	0	0	0	0	0	1	0	0	0	
86	0	0	0	0	0	1	0	1	0	1	0	0	0	
88	0	0	0	0	0	1	2	4	4	0	0	0	0	
90	0	0	0	1	5	20	31	23	3	0	0	0	0	
92	0	0	2	5	23	94	152	16	0	0	0	0	0	
94	0	0	2	6	12	43	139	18	0	0	0	0	0	
96	0	0	0	0	1	3	10	4	1	0	0	0	0	
98	0	0	0	0	1	0	0	0	0	0	0	0	0	
100	0	0	0	0	0	0	0	2	0	0	0	0	0	
102	0	0	0	0	0	0	0	0	0	0	0	0	0	
104	0	0	0	0	0	0	0	0	0	0	0	0	0	

(y)

(b)

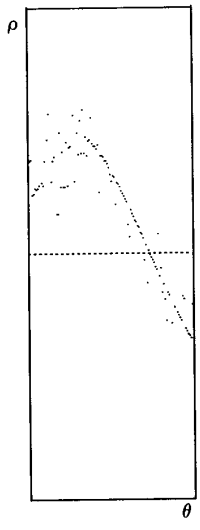

(c)

	122	124	126	128	130	132	134	136	138	140	142	144	146	(x)
104	0	2	0	1	0	0	0	0	0	0	0	0	1	
106	0	0	0	0	0	0	0	0	0	0	0	0	0	
108	0	0	0	0	0	0	0	0	0	0	0	0	0	
110	0	0	0	3	1	0	2	0	0	0	0	1	0	
112	0	0	0	0	4	0	0	0	0	0	0	0	0	
114	0	0	0	0	2	12	4	0	0	0	0	0	0	
116	0	0	0	0	5	34	59	13	1	1	0	0	0	
118	0	0	0	0	0	17	27	10	10	6	1	0	0	
120	0	0	0	0	1	3	13	2	3	0	0	1	0	
122	0	0	0	0	0	0	3	0	0	0	0	0	0	
124	0	0	0	0	0	0	0	0	0	0	1	0	0	
126	2	0	0	0	0	0	1	2	0	0	2	0	0	
128	0	0	0	0	2	1	0	0	0	0	0	0	0	

(y)

(d)

Fig. 9. (a) Translation term obtained by eliminating the intrinsic transform of S1; (b) translation term obtained by eliminating the intrinsic transform of S2; (c) Results of voting on the x-y plane using the translation term in (a); (d) results of voting on the x-y plane using the translation term in (b).

Conceptually, the amount of computation required to obtain the SLHT transform is of the same order of magnitude as computing the ψ-S representation. At each point along the curve boundary, once the slope is known, the tangent line at that point can also be obtained with a few arithmetic operations. Computation of the STIRS signature from the SLHT transform can be done efficiently. The major advantage of the STIRS signature over the ψ-S representation and the shape number is that the latter cannot be easily extended to cope with composite shapes and occlusion.

The proposed method can be further generalized to deal with large images. Suppose the test image T is divided into a set of (possibly overlapping) subimages $\{T_i\}$, and the reference image is divided into a set of subimages $\{R_j\}$. The SLHT transform and the (partial) signature of individual subimages are computed separately. Then, the partial signature of each subimage T_i is matched against the partial signatures of the reference subimages. If the signature of T_i matches with that of R_j, then we merge T_i with one of its neighbors, say T_i', and compute the new combined partial signature for $T_i \cup T_i'$. Note that the SLHT transform of the combined subimage can be obtained by combining the SLHT transforms of individual subimages. The same is done to the reference pattern. If the two new partial signatures match, then the merging will be accepted. When the partial test image reaches a certain size and the degree of correlation between the test and reference signature is greater than certain threshold, then we can proceed to verify the hypothesis and estimate the location of the test pattern.

III. Uniqueness of the SLHT Transform

In the pattern recognition methodology presented in Section II, it is assumed that the shapes are being represented by a set of tangents. One fundamental question we want to ask is the uniqueness of this representation. In this section, we will prove that in the continuous domain, the complete set of tangents of a planar closed smooth curve is indeed unique, provided the curve also satisfies a finiteness assumption listed below. This problem is also of interest in geometry, where it is known as the uniqueness problem [8]. The theorem proved in this section will serve as the theoretical basis of the recognition methodologies that are based on the SLHT. Comparisons of our work with that of Horwitz and with that of McKenzie will be discussed in Section III-C.

A. Main Theorem

Two basic assumptions are made:

Assumption 1

(Smoothness assumption): The curve C is continuous, smooth, simple, and closed.

Assumption 2

(Finite tangency): Let $T(C)$ be the set of straight lines that are tangent to C. There are only finitely many lines in $T(C)$ that have the same inclination. In other words, in any given direction, there are only a finite number of lines that are tangent to C.

If $T(C)$ satisfies Assumption 2, then we will be able to uniquely reconstruct C from $T(C)$ without knowing the point(s) of tangency on each tangent line (as shown later in this section). This implies that if two curves have the same set of tangents, then they have to be identical. Some previous studies on shape reconstruction from tangent lines (supporting lines) are restricted to the reconstruction of the convex hull [13], [18].

First, we will introduce some preliminaries and notations. A curve C in the x-y plane can be expressed as

$$C = C(s) = (x(s), y(s))$$

where s is the arc length measured along C in the counterclockwise direction from a reference point o (which is an arbitrary point on C). Thus, $(x(s), y(s))$ define a moving point in the x-y plane when the curve C is traversed. If C is smooth, then the first derivatives $x'(s)$ and $y'(s)$ exist and will not be both equal to zero for any s.

Let the line L_s be tangent to C at the point $(x(s), y(s))$. The slope of L_s is

$$m_s = \tan\phi(s) = \frac{y'(s)}{x'(s)}$$

where $\phi(s)$ is the angle measured from the positive x axis to the line L_s. The range of $\phi(s)$ is from 0° to 180°. The line L_s can also be characterized by $(\theta(s), \rho(s))$

$$L_s : \rho(s) = x\cos\theta(s) + y\sin\theta(s)$$

where $\rho(s)$ is the perpendicular distance of the origin from L_s, and $\theta(s)$ is the angle measured from the positive x axis to the line normal to L_s. We have the slope of the normal

$$\tan\theta(s) = \frac{-x'(s)}{y'(s)}.$$

We can also observe that $\phi(s)$ and $\theta(s)$ are related by

$$\theta(s) = (\phi(s) + 90°) \pmod{180}, \text{ and}$$
$$\phi(s) = (\theta(s) + 90°) \pmod{180}.$$

The pair $(\theta(s), \rho(s))$ defines a corresponding moving point in the θ-ρ space.[3]

[3]Every straight line in the x-y plane is uniquely represented by a point in the θ-ρ space except for vertical lines. A vertical line $x = a$ is mapped to two points $(0°, a)$ and $(180°, -a)$ in θ-ρ space.

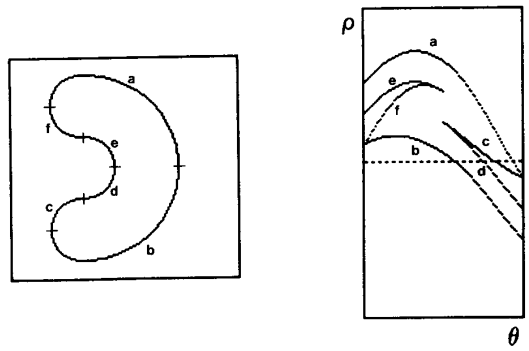

Fig. 10. Shape S1 and its H transform.

Definition

Transformation H: Suppose we traverse the curve C in the counterclockwise direction, and compute the tangent line to C at $(x(s), y(s))$ and the corresponding moving point $(\theta(s), \rho(s))$ in the θ-ρ space. The resultant *pattern* traced by the moving point $(\theta(s), \rho(s))$ is denoted as $H(C)$.

Although $H(C)$ is obtained from the trace of $(\theta(s), \rho(s))$, it is represented by the set of points visited by $(\theta(s), \rho(s))$.

Main Theorem: For two curves C_1 and C_2 that satisfy Assumptions 1 and 2, $H(C_1) = H(C_2)$ if and only if $C_1 = C_2$.

1) Outline of the Proof: We will prove the theorem by showing that given $H(C)$, the original curve C can be uniquely reconstructed. Fig. 10 shows a shape S1 and its H transform. We can observe that the H transform of the curve is composed of a set of continuous branches in θ-ρ, where a branch is a continuous curve in θ-ρ such that it does not intersect or touch other branches except at its two end points. The formal definition of the branches will be given in the next section. Each of the branches corresponds to a convex or concave curve segment of S1. The branches and the curve segments are labeled in Fig. 10. Applying the theory of convexity, we can reconstruct the epigraph of the convex/concave region corresponding to the convex/concave curve from its complete set of tangents. A *reduced* version of the convex/concave curve is then obtained by removing the two semi-tangents of the boundary of the epigraph. Let F be a convex/concave curve, and let F_r be the *reduced* version of F. F_r is equivalent to the curve obtained by removing the points of F that are lying on the two semi-tangents to F at its two end points.

If the given shape satisfies assumptions 1 and 2, then its H transform can always be decomposed into a unique finite set of branches. From each of the branches, we can reconstruct the epigraphs and the *reduced* convex/concave curve segments. To reconstruct the shape, we only need to connect the pairs of end points of the convex/concave segments. By continuity, there is only one possible way to connect the pairs of end points to obtain a simple closed smooth curve. This implies that the reconstructed shape is unique and must be equal to the original shape.

2) Details of the Proof: First, we consider some of the properties of $H(C)$.

$$L_a^+ = \begin{cases} L_a & \text{if } L_a \text{ is nonvertical} \\ \{(x,y)|(x,y) \in L_a \text{ and } y \geq F(a)\} & \text{if } L_a \text{ is vertical and } F \text{ is convex} \\ \{(x,y)|(x,y) \in L_a \text{ and} y \leq F(a)\} & \text{if } L_a \text{ is vertical and } F \text{ is concave} \end{cases}$$

Lemma 1: If C satisfies Assumption 1, then the following holds:

1. The trace of the moving point $(\theta(s), \rho(s))$ in the θ-ρ space is continuous, except that there is a discontinuity jump from some point $(180°, -a)$ to the point $(0°, a)$, and vice versa.
2. $(\theta(s), \rho(s))$ will not move vertically.

Proof: Recall that $\tan\theta(s) = -x'(s)/y'(s)$, and $\rho(s) = x(s)\cos\theta(s) + y(s)\sin\theta(s)$. Since C is continuous and smooth

$$\lim_{s_1 \to s_0} x'(s_1) \to x'(s_0), \text{ and } \lim_{s_1 \to s_0} y'(s_1) \to y'(s_0).$$

To show 1), we consider the following three cases separately.

a) $y'(s_0) \neq 0$ and $x'(s_0) \neq 0$.

For any point s_1, it is easy to observe that

$$\lim_{s_1 \to s_0} \theta(s_1) \to \theta(s_0), \text{and } \lim_{s_1 \to s_0} \rho(s_1) \to \rho(s_0).$$

b) $y'(s_0) \neq 0$ and $x'(s_0) = 0$.

In this case, the tangent is a vertical line. This line is mapped to the two points $(0°, x(s_0))$ and $(180°, -x(s_0))$ in $\theta - \rho$.

For s_1 such that $x'(s_1) > 0$

$$\lim_{s_1 \to s_0} \theta(s_1) \to 180° \text{and} \lim_{s_1 \to s_0} \rho(s_1) \to -x(s_0) \text{ if } y'(s_0) > 0,$$

$$\lim_{s_1 \to s_0} \theta(s_1) \to 0° \text{and} \lim_{s_1 \to s_0} \rho(s_1) \to x(s_0) \text{ if } y'(s_0) < 0.$$

For s_1 such that $x'(s_1) < 0$

$$\lim_{s_1 \to s_0} \theta(s_1) \to 0° \text{and} \lim_{s_1 \to s_0} \rho(s_1) \to x(s_0) \text{ if } y'(s_0) > 0,$$

$$\lim_{s_1 \to s_0} \theta(s_1) \to 180° \text{and} \lim_{s_1 \to s_0} \rho(s_1) \to -x(s_0) \text{ if } y'(s_0) < 0.$$

c) $y'(s_0) = 0$ and $x'(s_0) \neq 0$.

In this case, the tangent is a horizontal line that is mapped to $(90°, y(s_0))$.

For s_1 such that $y'(s_1) > 0$

$$\lim_{s_1 \to s_0} \theta(s_1) \to 90°^+ \text{if } x'(s_0) > 0,$$

$$\lim_{s_1 \to s_0} \theta(s_1) \to 90°^- \text{if } x'(s_0) < 0.$$

For s_1 such that $y'(s_1) < 0$

$$\lim_{s_1 \to s_0} \theta(s_1) \to 90°^- \text{if } x'(s_0) > 0,$$

$$\lim_{s_1 \to s_0} \theta(s_1) \to 90°^+ \text{if } x'(s_0) < 0.$$

In both cases

$$\lim_{s_1 \to s_0} \rho(s_1) \to y(s_0).$$

To show 2), we will derive a contradiction. Without loss of generality, assume that $(\theta(s), \rho(s))$ moves vertically upward (or downward) at $\theta = 90°$ for some $s \in [s_0, s_1]$. Recall that $\tan\theta(s) = -x'(s)/y'(s)$. If $\theta(s) = 90°$, then $y'(s) = 0$. This implies that the corresponding curve segment $C(s)$ for $s \in [s_0, s_1]$ should be a horizontal line. Hence, $\rho(s)$ cannot move upward (or downward) for $s \in [s_0, s_1]$. □

Before we present the reconstruction of general smooth closed curves, we first consider the reconstruction of simple open convex (or concave) curves. Let $F = F(x)$ for $x \in [a, b]$ be a single valued function[4] that is continuous and smooth.

Lemma 2: If $H(F)$ is a single continuous curve in θ-ρ such that 1) $0° \leq \theta \leq 180°$ and 2) no two points in $H(F)$ possess the same θ value, then F is either convex or concave.

Proof: $H(F)$ is the set of points visited by the moving point $(\theta(s), \rho(s))$ when F is traversed. In this particular case since no two points in $H(F)$ can have the same θ value, $\theta(s)$ must be monotonic in s. Suppose $\theta(s)$ is monotonically increasing in s. Since $\phi = (\theta + 90°) \text{mod} 180$

$$\lim_{\theta \to 0^+} \phi \to 90°^+ \Rightarrow \tan\phi \to -\infty$$

$$\lim_{\theta \to 90°} \phi \to 0° \Rightarrow \tan\phi \to 0$$

$$\lim_{\theta \to 180°^-} \phi \to 90°^- \Rightarrow \tan\phi \to +\infty.$$

Hence, $F'(x)$ is nondecreasing in $a \leq x \leq b$. Therefore, $F(x)$ is convex (see Theorem 4.4 of [16]). Similarly, if $\theta(s)$ is monotonically decreasing in s, then $F(x)$ is concave. □

In the following discussion, F is assumed to be either convex or concave.

Definitions: Let $(a, F(a))$ and $(b, F(b))$ be the two end points of F. Let L_a and L_b be the two tangent lines to F at its two end points, respectively. The *extended curve* F_e is defined as follows:

$$F_e = \begin{cases} L_a^+ & \text{for } x \leq a \\ F & \text{for } a < x < b \\ L_b^+ & \text{for } x \geq b \end{cases}$$

where L_a^+ is defined at the top of this page and where and L_b^+ is defined similarly. The *domain* of F_e denoted as Dom_{F_e} is defined as follows:

$$Dom_{F_e} = \begin{cases} (-\infty, +\infty) & \text{if } L_a \text{ and } L_b \text{ are nonvertical} \\ (-\infty, b] & \text{if } L_a \text{ is nonvertical and } L_b \text{ is vertical} \\ [a, +\infty) & \text{if } L_a \text{ is vertical and } L_b \text{ is nonvertical} \\ [a, b] & \text{if } L_a \text{ and } L_b \text{ are vertical.} \end{cases}$$

[4]The terms "curve" and "function" are used synonymously in this section.

The *epigraph* of F_e denoted epi_{F_e} is defined at the bottom of this page. Hence, the boundary of $epi_{F_e} \triangleq F_e$. Let a' and b' be two x's such that

1. $a' \geq a$ and $b' \leq b$.
2. The point $(a', F(a'))$ lies on L_a and $(b', F(b'))$ lies on L_b.
3. For $x \in (a', b')$, $(x, F(x))$ does not lie on either L_a or L_b.

Then, the *reduced curve* F_r is defined as

$$F_r = F \text{ for } x \in [a', b'].$$

It is easy to see that $H(F) = H(F_e) = H(F_r)$.

Lemma 3: If $F(x)$ is defined for $x \in [a, b]$ and $F(x)$ is convex or concave, then F_e can be uniquely reconstructed from $H(F)$.

Proof: From the study of convexity [3], [16], every tangent line to F_e defines a supporting half plane for epi_{F_e}. Moreover, epi_{F_e} can be uniquely determined by taking the intersection of all the supporting half planes defined by the set of tangents to F_e (see Theorem 7.8 of [3]). To apply these results, we need only to determine whether F is convex or concave from $H(F)$ and then determine the supporting half planes of each tangent line.

Let the range of θ in $H(F)$ be $[\theta_s, \theta_e]$ and $\theta_e > \theta_s$. Select three tangent lines L_a, L_b, and L_c such that $\theta_s < \theta_a < \theta_b < \theta_c < \theta_e$. We first reconstruct L_a and L_c in the x-y plane. These two lines will meet at some point p and divide the x-y plane into four regions r_1, r_2, r_3, and r_4 (Fig. 11) such that

$$\begin{aligned}
r_1 &= \{(x,y) | x\cos\theta_a + y\sin\theta_a \leq \rho_a \text{ and } x\cos\theta_c + y\sin\theta_c \leq \rho_c\},\\
r_2 &= \{(x,y) | x\cos\theta_a + y\sin\theta_a \geq \rho_a \text{ and } x\cos\theta_c + y\sin\theta_c \leq \rho_c\},\\
r_3 &= \{(x,y) | x\cos\theta_a + y\sin\theta_a \geq \rho_a \text{ and } x\cos\theta_c + y\sin\theta_c \geq \rho_c\},\\
r_4 &= \{(x,y) | x\cos\theta_a + y\sin\theta_a \leq \rho_a \text{ and } x\cos\theta_c + y\sin\theta_c \geq \rho_c\}.
\end{aligned}$$

If F is convex, then F must lie within r_3. If F is concave, then F must lie within r_1.

Now, consider line L_b. Note that L_b cannot pass through the point p. If L_b passes through point p, then p is the only point in the intersection of r_1 and L_b (or r_3 and L_b). Hence, L_b must be tangent to F at point p. However, L_a and L_c are also valid tangent lines at point p, which violates the assumption that F is a smooth curve. Hence, L_b can only pass through r_1 or r_3 (not both). If L_b passes through r_1, then F must lie within r_1, and hence, it is concave. If L_b passes through r_3, then F must lie within r_3 and is convex. □

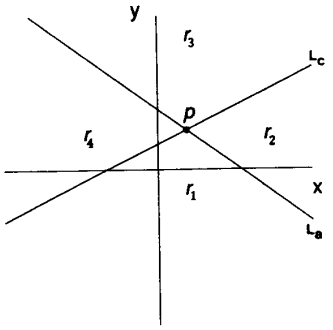

Fig. 11. Partition of the x-y plane by two nonparallel lines.

Now, we consider the implications of the second assumption on $H(C)$. First, we introduce the following definitions.

Definition: A *branch* in $H(C)$ is a maximal subset of $H(C)$ such that the following occurs:

1. It is a continuous curve for $0° \leq \theta \leq 180°$.
2. No two points in the subset have the same θ value.
3. If point q belongs to branch B_i, then q does not belong to any other branch B_j, unless q is the end point of B_i. The end point of a branch is the point that has the smallest or largest value of θ in that branch.

Lemma 4: If C satisfies Assumption 2, then the following statements hold:

1. C is formed by the concatenation of a finite number of convex/concave curve segments.
2. There are only a finite number of common tangent lines (lines tangent to C at more than one disjoint intervals of s).
3. $H(C)$ does not occupy any filled region in θ-ρ.

Proof: 1) By Lemma 2, a convex/concave curve segment is transformed into a continuous curve in θ-ρ with $0° \leq \theta \leq 180°$. For any given θ, there are only a finite number of distinct ρ's. Hence, $H(C)$ contains only a finite number of curves.

2) We will show that given two convex/concave segments F_1 and F_2, they can have, at most, two nonvertical common tangents.

a. Assume F_1 is convex, and F_2 is concave. Suppose lines L_a and L_c are the two common tangents. These two lines will divide the x-y plane into four regions as in the proof of Lemma 3. F_1 should be contained in r_3, and F_2 should be within r_1. For any other nonvertical line that is tangent to either F_1 or F_2, it can only pass through either r_1 or r_3 but not both.

b. Assume both F_1 and F_2 are convex. In this case, F_1 cannot touch F_2,; otherwise, C is not a simple curve. Suppose lines L_a and L_c are the two common tangents. Both F_1 and F_2 have to be within region r_3. Assume

$$epi_{F_e} = \begin{cases} \{(x,y) | x \in Dom_{F_e} \text{ and } y \geq F_e(x)\} & \text{if } F \text{ is convex} \\ \{(x,y) | x \in Dom_{F_e} \text{ and } y \leq F_e(x)\} & \text{if } F \text{ is concave.} \end{cases}$$

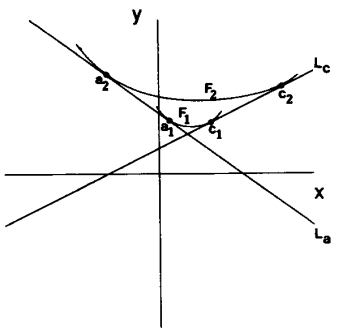

Fig. 12. Common tangents of two convex curves.

$F_2 > F_1$ for all $x \in Dom_{F_1} \cap Dom_{F_2}$. Let L_a be tangent to F_1 at $x = a_1$, and let L_c be tangent to F_1 at $x = c_1$ (refer to Fig. 12). Since $F_2 > F_1$ for all $x \in [a_1, c_1]$, the points of tangency of L_a and L_c to F_2, namely a_2 and c_2, respectively, should satisfy $a_2 < a_1$, and $c_2 > c_1$. Now, consider line L_b.

i. $\theta_a < \theta_b < \theta_c$: L_b cannot be tangent to both F_1 and F_2. Otherwise, F_1 will be equal to F_2 at the point of tangency to F_1.

ii. $\theta_b < \theta_a$: If L_b is tangent to F_2, then it must intersect L_a to the left of a_2. Hence, L_b cannot be tangent to F_1. If L_b is tangent to F_1, then it must intersect L_a in between a_1 and a_2. Hence, L_b cannot be tangent to F_2.

iii. $\theta_b > \theta_c$: This is similar to case ii.

c. Assume both F_1 and F_2 are concave. This is similar to case b.

4) Suppose $H(C)$ occupies a filled region $\{(\rho,\theta)|\rho \in [\rho_1, \rho_1 + \Delta\rho]$ and $\theta \in [\theta_1, \theta_1 + \Delta\theta]\}$. Then, at $\theta = \theta_1 + \delta$ for $0 < \delta < \Delta\theta$, there are infinite ρ's, contradicting Assumption 2. □

Lemma 5: If the line $L_1 = (\theta_1, \rho_1)$ is tangent to $C(s)$ at k disjoint intervals $\{I_1 = [s_{11}, s_{12}]$, $I_2 = [s_{21}, s_{22}], \ldots,$ $I_k = [s_{k1}, s_{k2}]\}$, then there are $2k$ branches in $H(C)$ that meet at (θ_1, ρ_1). If $\theta_1 = 0°$ (or 180°), then the branch with the end point at $(180°, -\rho_1)$ (or $(0°, -\rho_1)$) is considered to be connected to (θ_1, ρ_1).

Proof: Suppose we traverse C starting from a point not belonging to any of the k intervals. In one complete traversal of C, the corresponding moving point $(\theta(s), \rho(s))$ in θ-ρ will visit the point (θ_1, ρ_1) k times, i.e., $(\theta(s), \rho(s))$ will move into and out of (θ_1, ρ_1) k times. Hence, there are $2k$ branches meeting at (θ_1, ρ_1). In the special case when $\theta_1 = 0°$ (or 180°), the moving point $(\theta(s), \rho(s))$ will jump to $(180°, -\rho_1)$ (or $(0°, -\rho_1)$).

Let B_i be the branch that was traced by $(\theta(s), \rho(s))$ when traversing an interval on C that is connected to I_i. The $2k$ branches have to be distinct. If these $2k$ branches are not distinct, say $B_i = B_j$, then the same segment in C is traversed more than once. This contradicts the assumption that C is a simple curve. □

Corollary 1: If C satisfies Assumptions 1 and 2, then a line L can be tangent to C at only a finite number of disjoint intervals.

Corollary 2: If C satisfies Assumptions 1 and 2, then $H(C)$ can always be decomposed into a unique set of finite branches $\{B_i\}$.

Proof of Main Theorem: If $C_1 = C_2$, then $H(C_1) = H(C_2)$. This part is trivial.

If $H(C_1) = H(C_2)$, then $C_1 = C_2$. To prove this, we will show that the curve C can be uniquely reconstructed from $H(C)$.

Given $H(C)$, we can always decompose it into a finite set of branches $\{B_i\}$ (by Corollary 2). For each branch B_i, we can reconstruct the epigraph of the convex/concave segment F_{e^i} (by Lemma 2). Hence, we can determine F_{r^i}, which is a subset of F_i. If point p belongs to F_i but not to F_{r^i}, then p must lie on the line that is tangent to F_i at one of its end points. Let $C_r{}'$ denote the union of all the F_{r^i}'s reconstructed.

For a given tangent line L_i, if L_i is tangent to C at intervals $[s_{11}, s_{12}], \ldots,$ $[s_{k1}, s_{k2}]$, then the points $C(s_{11}), C(s_{12}), \ldots, C(s_{k1})$, and $C(s_{k2})$ are in $C_r{}'$. Moreover, for all points $p_j = C(s_j)$, for $s_j \in (s_{j1}, s_{j2})$ for $j = 1$ to k, p_j lies on the straight line segment joining $C(s_{j1})$ and $C(s_{j2})$. If the original curve C is simple, then all the k straight line segments joining $C(s_{11})$ to $C(s_{12}), \ldots,$ and $C(s_{k1})$ to $C(s_{k2})$ must be disjoint and do not intersect other curve segments of C. Hence, those points in C but not in $C_r{}'$ satisfy the following condition:

If $p = C(s)$ for $s \in (s_1, s_2)$ and p belongs to C but not to $C_r{}'$, then p must lie on the straight line segment joining $C(s_1)$ to $C(s_2)$.

Hence, we can recover all the points in C but not in $C_r{}'$ by constructing straight line segments joining the end points in $C_r{}'$.

Consider the line $L_j = (\theta_j, \rho_j)$ such that (θ_j, ρ_j) is an end point of some branches. Let $P_j = \{p|p$ be an end point of some F_{r^i} and L_j be tangent to F_{r^i} at $p\}$. The number of points in P_j is always even (by Lemma 5). Let $P_j = \{p_1, p_2, \ldots, p_2k\}$ and the p_i's be sorted such that $x\_p_i \leq x\_p_j$ and $y\_p_i \leq y\_p_j$ for $i < j$, where x_p_i is the x coordinate of p_i, and y_p_i is the y coordinate of p_i. We then connect the pairs of points p_i to p_{i+1} for all i's that are odd. The reconstructed curve C_r is taken as the union of $C_r{}'$ and all the straight line segments joining pairs of end points in $C_r{}'$ as described. Note that C_r is closed since every end point in $C_r{}'$ is connected to exactly one other end point. In addition, C_r is simple since line segments connecting pairs of end points do not intersect.

By continuity, there is only one way, as described above, to join all the end points in $C_r{}'$ to obtain a simple closed smooth curve. Hence, C_r must equal C. □

B. Reconstruction of Open Smooth Curves

In the case of open curves, Lemma 5 may not hold in general. However, the reconstruction procedure can still be applied with the final step modified as follows. Given a convex/concave curve F, the two semi-infinite straight lines obtained by F_e-F_r are the two *semi-tangents* of F at its two

end points. To connect the end points in C_r', we need to consider the direction of extension of the semi-tangents at the end points of each concave/convex segment. Let L_a be a common tangent at the two points (x_1, y_1) and (x_2, y_2), which are end points of two curves F_{ri} and F_{rj}, respectively. Assume that $x_1 < x_2$ (or $y_1 < y_2$ if L_a is vertical). Suppose the semi-tangent at (x_1, y_1) extends in the direction of positive x (or positive y if L_a is vertical), and the semi-tangent at (x_2, y_2) extends in the direction of negative x. We will then connect (x_1, y_1) and (x_2, y_2) if and only if there is no other end point of some F_{rk} that lies in between (x_1, y_1) and (x_2, y_2). The reconstructed curve C_r is identical to the original curve C except for the two straight line segments at the two ends of C. Hence, C_r is a *reduced* version of C.

C. Comparisons with Horwitz's Proof and McKenzie's Work

During the course of our work, we became aware of the proof reported in [8]. Horwitz's work is in a slightly different context. He only considered functions of a single variable, i.e., open curves. His proof is based on the notion of convergence. A sequence of lines $\{L_i\}$ converges to L if i) the slope of L_i converges to the slope of L; ii) the y intercept of L_i converges to the y intercept of L. The point of tangency of L is equal to the limit point of the intersection of $\{L_i\}$ with L. Such a limit exists provided i) both the first and second derivatives of the function exist, and ii) the second derivative is equal to zero at most a finite number of times. However, for common tangents,[5] the limit point is not unique. Horwitz resolved this problem by simply ignoring all common tangents in his reconstruction procedure. He argued that if there are only a *finite* number of common tangents, then the finite number of points not reconstructed can be recovered by continuity constraints. The following implications can be derived from the assumptions:

1. There are only a finite number of points of inflection on the curve.
2. There are only a finite number of common tangents.[6]
3. There is no straight line segment in the curve.[7]

Our proof is based on the reconstruction of the epigraph of a convex/concave curve from its supporting half planes. We make no assumption on the second derivative of the curve, and we are able to reconstruct every point (including straight line segments) of the original curve if the curve is closed. If the curve is open, we can reconstruct the *reduced* version of the original.

Both Horwitz's method and our method are restricted to finite curves. In the case of infinite curves, i.e., an infinite spiral, the trace of $(\theta(s), \rho(s))$ will eventually fill up a region in θ-ρ. Hence, we will no longer be able to decompose $H(C)$ into a set of distinct branches. Horwitz's reconstruction procedure will also fail because there are an infinite number of common tangents.

McKenzie and Protheroe described a method to reconstruct curves from the θ-ρ space [12]. They showed that if the curve in the θ-ρ space is differentiable (which implies that the second derivative of the curve C exists), then the point of tangency of the line to the curve C can be computed. Because of the above assumption, the same limitation of Horwitz method applies.

IV. Concluding Remarks and Future Research

Even though shape matching is a conceptually simple problem, its time complexity is enormous. In order to bring down the complexity, we need to decompose the high dimensional parameter space into several lower dimensional subspaces such that parameters of individual subspaces can be determined sequentially. The SLHT transform offers a natural way to decompose the parameter space into three subspaces, namely, the translation space, rotation space, and the intrinsic space.

The use of SLHT in shape recognition has been studied previously in [5], [12], and [14]. By proving the uniqueness of the SLHT transform of closed smooth curves, we establish a solid theoretical foundation of the methodology.

The second major contribution of this paper is the generalization of the approach, and the introduction of the scalable translation invariant rotation-to-shifting (STIRS) signature. As the name implies, the signature is scalable and invariant to translation, and rotation in image space corresponds to circular shifting of the signature space. Matching in this signature space only involves computing a 1-D correlation of the reference template with the test template. Although the STIRS signature is not unique, for nontrivial shapes, the existence of the peak in the correlation gives a strong indication of the likelihood of the presence of the reference object in the test image. The location of the peak also indicates the orientation of the test object. Knowing the orientation information of the test object, we can obtain the translation term of the SLHT transform of the test object by subtracting the intrinsic term from the transform. This subtraction operation is equivalent to computing a column-by-column correlation between the reference transform and the test transform. The location of the test object is then computed by an inverse transform (or voting) from the θ-ρ space to the x-y plane.

The examples presented in Section II-C demonstrate the feasibility of the method. One important issue that would require further research is the sensitivity of the STIRS signature to composite shapes, distortion, and occlusion. To understand the sensitivity of the signature, we have to analyze the "shape" features that are being captured. A convex/concave segment is also mapped to a continuous curve in θ-ρ. The number of points in θ-ρ does not depend directly on the length of the contour. It is instead proportional to the angular span of the curve, and the pattern in θ-ρ depends on the curvature and position of the curve segments in the image plane. The signature is obtained by measuring the perpendicular distances between pairs of parallel tangents. It captures the relative position of a curve segment with respect to other curve

[5] In [8], a common tangent (multiple tangent as used in [8]) is defined as a line that is tangent to the curve at more than one point.

[6] This is true only for single valued functions. For closed curves or general 2-D curves, such as an infinite spiral, there can be an infinite number of common tangents even if the second derivative equals zero finite number of times.

[7] The difficulty in dealing with straight line segments in Horwitz's reconstruction procedure is due to the fact that the end points of the straight line segments cannot be determined.

segments of the shape contour. When there are multiple shapes in the image, the STIRS signature may capture characteristics of spurious shapes, such as the convex hull of the composite shape, and the shapes formed by the intersections of the contours of the constituent shapes. The correlator may raise false alarms when matching shapes that are similar to any one of the spurious shapes. However, this is a common problem to all shape matching methods, irrespective of the shape measures used. In general, the interference between two shapes tend to decrease when the two shapes are further apart from each other. One major reason is that the composite STIRS signature will be stretched and will become "taller." The density of the points in the lower region (smaller ρ values) will decrease. If the size of the test object is known, we can also clip the STIRS signature by discarding points with ρ values that are larger than the diameter of the reference object.

Distortions and occlusion will lead to displacement or removal of points in the θ-ρ space. Hence, the amount of distortion or occlusion that can be tolerated depends on the amount of changes to the angular span of the object contour instead of changes in the number of contour pixels (or area).

Another issue related to occlusion is missing segments of the object contour. For example, in character recognition, if part of the character with less dominant features are missing, the STIRS signature may still perform well as in some (but not all) other shape measures.

ACKNOWLEDGMENT

The authors would like to thank Dr. L. Lam and S. Y. Leung for their constructive comments and stimulating discussion. The valuable suggestions and comments of the referees are very much appreciated.

REFERENCES

[1] D. H. Ballard, "Generalizing the Hough transform to detect arbitrary shapes," *Patt. Recogn.*, vol. 13, pp. 111–122, 1981.
[2] D. H. Ballard and C. M. Brown, *Computer Vision*. Englewood Cliffs, NJ: Prentice-Hall, 1982.
[3] R. V. Benson, *Euclidean Geometry and Convexity*. New York: McGraw-Hill, 1966.
[4] E. Bribiesca and A. Guzman, "How to describe pure form and how to measure differences in shapes using shape numbers," in *Proc. IEEE Conf. Patt. Recogn. Image Processing*, 1979, pp. 427–436.
[5] D. Casasent and R. Krishnapuram, "Curved object location by Hough transformations and inversions," *Patt. Recogn.*, vol. 20, no. 2, pp. 181–188, 1987.
[6] G. D. Chakerian, "A characterization of curves of constant width," *Amer. Math. Monthly*, vol. 81, pp. 153–155, 1974.
[7] R. O. Duda, P. E. Hart, "Use of the Hough transformation to detect lines and curves in pictures," *Comm. ACM*, vol. 15, no. 1, pp. 11–15 1972.
[8] A. Horwitz, "Reconstructing a function from its set of tangent lines," *Amer. Math. Monthly*, vol. 96, no. 9, pp. 807–813, Nov. 1989.
[9] J. Illingworth and J. Kittler, "A survey of the Hough transform," *Comput. Vision Graphics Image Processing*, vol. 44, no. 1, pp. 87–116, 1988.
[10] R. Krishnapuram and D. Casasent, "Hough space transformations for discrimination and distortion estimation," *Comput. Vision Graphics Image Processing*, vol. 38, pp. 299–316, 1987.
[11] H. F. Li, D. Pao, and R. Jayakumar, "Improvements and systolic implementation of the Hough transformation for straight line detection," *Patt. Recogn.*, vol. 22, no. 6, pp. 697–706, 1989.
[12] D. S. McKenzie and S. R. Protheroe, "Curve description using the inverse Hough transform," *Patt. Recogn.*, vol. 23, nos. 3 and 4, pp. 283–290, 1990.
[13] K. Murakami, H. Koshimizu, and K. Hasegawa, "An algorithm to extract convex hull on θ-ρ transform space," in *Proc. Int. Conf. Patt. Recogn.*, 1988, pp. 500–503.
[14] D. Pao, H. F. Li, and R. Jayakumar, "Detecting parametric curves using the straight line Hough transform," in *Proc. Int. Conf. Patt. Recogn.*, June 1990, pp. 620–625.
[15] ——, "A decomposable parameter space for the detection of ellipses," to be published in *Patt. Recogn. Lett.*
[16] R. T. Rockafellar, *Convex Analysis*. Princeton, NJ: *Princeton University Press*, 1970.
[17] T. M. van Veen and F. C. A. Groen, "Discretization errors in the Hough transform," *Patt. Recogn.*, vol. 14, pp. 137–145, 1981.
[18] J. L. Prince and A. S. Willsky, "Reconstructing convex sets from support line measurements," *IEEE Trans. Patt. Anal. Machine Intell.*, vol. 12, no. 4, pp. 377–389, 1990.
[19] S. Tsuji and F. Matsumoto, "Detection of ellipses by a modified Hough transform," *IEEE Trans. Comput.*, vol. 27, pp. 777–781, 1978.

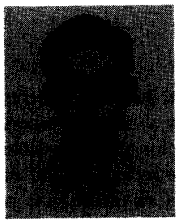

Derek C. W. Pao received the B.Sc.(Eng.) degree in electrical engineering from the University of Hong Kong in 1984 and the M. Comp. Sci. and Ph.D. degrees in computer science from Concordia University, Montreal, Canada, in 1987 and 1991, respectively.

From July 1984 to December 1985, he was with RCL Semiconductors Ltd., Hong Kong, as a design engineer. Currently, he is a Visiting Assisitant Professor of Computer Science at Concordia University. His research interests include pattern recognition and image processing, VLSI algorithms and architectures, and parallel processing.

Hon F. Li (S'73–M'75) received the B.S. degree (with highest honors) in 1972 from the University of California, Berkeley, and the Ph.D. degree in the area of parallel-pipelined computer architecture in 1975.

He subsequently joined the University of Illinois, Urbana-Champaign, as an Assistant Professor in the Computer Engineering Group, Department of Electrical Engineering. He went to Hong Kong in 1977 and served as Lecturer and, later, Senior Lecturer in the Department of Electrical Engineering, University of Hong Kong, where he developed both an undergraduate and a graduate program in computer engineering. In 1984, he joined Concordia University, Montreal, Canada, where he is now a Professor of Computer Science. His research interests cover the general areas of parallel and distributed processing, VLSI algorithms and architectures, and system specification.

R. Jayakumar received the B.E.(Hon's) degree in electronics and communication engineering from the University of Madras, Madras, India, in 1977, the M.S. degree in computer science from the Indian Institute of Technology, Madras, India, in 1980, and the Ph.D. degree in engineering and computer science from Concordia University, Montreal, Canada, in 1984.

His research interests are in VLSI algorithms and architectures, fault-tolerant VLSI systems, VLSI design automation, and graph theory and graph algorithms.

Dr. Jayakumar is a member of the Association for Computing Machinery and the IEEE Computer Society.